



Article

Plasma Level of Pyrophosphate Is Low in Pseudoxanthoma Elasticum Owing to Mutations in the ABCC6 Gene, but It Does Not Correlate with ABCC6 Genotype

Eszter Kozák ^{1,†}, Jonas W. Bartstra ^{2,†}, Pim A. de Jong ², Willem P. T. M. Mali ², Krisztina Fülöp ¹, Natália Tőkési ¹, Viola Pomozi ¹, Sara Risseuw ³, Jeannette Ossewaarde-van Norel ³, Redmer van Leeuwen ³, András Váradi ^{1,‡} and Wilko Spiering ^{4,*} 

¹ Institute of Enzymology, Research Center for Natural Sciences, Hungarian Academy of Sciences Center of Excellence, 1117 Budapest, Hungary

² Department of Radiology, University Medical Center Utrecht, Utrecht University, 3584 CX Utrecht, The Netherlands

³ Department of Ophthalmology, University Medical Center Utrecht, Utrecht University, 3584 CX Utrecht, The Netherlands

⁴ Department of Vascular Medicine, University Medical Center Utrecht, Utrecht University, 3584 CX Utrecht, The Netherlands

* Correspondence: w.spiering@umcutrecht.nl; Tel.: +31-88-7571188

† These authors contributed equally to this work.

‡ These authors contributed equally to this work.



Citation: Kozák, E.; Bartstra, J.W.; de Jong, P.A.; Mali, W.P.T.M.; Fülöp, K.; Tőkési, N.; Pomozi, V.; Risseuw, S.; Norel, J.O.-v.; van Leeuwen, R.; et al. Plasma Level of Pyrophosphate Is Low in Pseudoxanthoma Elasticum Owing to Mutations in the ABCC6 Gene, but It Does Not Correlate with ABCC6 Genotype. *J. Clin. Med.* **2023**, *12*, 1047. <https://doi.org/10.3390/jcm12031047>

Academic Editor: Carmelo Bernabeu

Received: 4 November 2022

Revised: 4 January 2023

Accepted: 22 January 2023

Published: 29 January 2023



Copyright: © 2023 by the authors. Licensee MDPI, Basel, Switzerland. This article is an open access article distributed under the terms and conditions of the Creative Commons Attribution (CC BY) license (<https://creativecommons.org/licenses/by/4.0/>).

Abstract: Background: Pseudoxanthoma elasticum (PXE), a monogenic disorder resulting in calcification affecting the skin, eyes and peripheral arteries, is caused by mutations in the ABCC6 gene, and is associated with low plasma inorganic pyrophosphate (PP_i). It is unknown how ABCC6 genotype affects plasma PP_i. Methods: We studied the association of ABCC6 genotype (192 patients with biallelic pathogenic ABCC6 mutations) and PP_i levels, and its association with the severity of arterial and ophthalmological phenotypes. ABCC6 variants were classified as truncating or non-truncating, and three groups of the 192 patients were formed: those with truncating mutations on both chromosomes ($n = 121$), those with two non-truncating mutations ($n = 10$), and a group who had one truncating and one non-truncating ABCC6 mutation ($n = 61$). The hypothesis formulated before this study was that there was a negative association between PP_i level and disease severity. Results: Our findings confirm low PP_i in PXE compared with healthy controls (0.53 ± 0.15 vs. 1.13 ± 0.29 μM , $p < 0.01$). The PP_i of patients correlated with increasing age (β : 0.05 μM , 95% CI: 0.03 – 0.06 per 10 years) and was higher in females (0.55 ± 0.17 vs. 0.51 ± 0.13 μM in males, $p = 0.03$). However, no association between PP_i and PXE phenotypes was found. When adjusted for age and sex, no association between PP_i and ABCC6 genotype was found. Conclusions: Our data suggest that the relationship between ABCC6 mutations and reduced plasma PP_i may not be as direct as previously thought. PP_i levels varied widely, even in patients with the same ABCC6 mutations, further suggesting a lack of direct correlation between them, even though the ABCC6 protein-mediated pathway is responsible for ~60% of this metabolite in the circulation. We discuss potential factors that may perturb the expected associations between ABCC6 genotype and PP_i and between PP_i and disease severity. Our findings support the argument that predictions of pathogenicity made on the basis of mutations (or on the structure of the mutated protein) could be misleading.

Keywords: pseudoxanthoma elasticum; PXE; genotype-phenotype association; plasma pyrophosphate; ectopic mineralization

1. Introduction

Physiological calcification is regulated through a complex network of calcification promoters and inhibitors which are finely tuned to confine calcification to the bones [1] and

prevent pathological soft tissue calcification. Inorganic pyrophosphate (PP_i) is a strong inhibitor of ectopic calcification and the effect of its dysregulation is demonstrated in pseudoxanthoma elasticum (PXE, OMIM 264800) [2,3], a model disease of soft tissue calcification.

Due to mutations in the ABCC6 gene, PXE patients have markedly reduced levels of circulating PP_i and as a consequence, ectopic calcification develops in multiple organs [2]. In the skin, calcification results in plaques and papules known as pseudoxanthomas [4]. Calcification of Bruch's membrane underlies peau d'orange and angioid streaks in the eye, which cause considerable visual morbidity due to choroidal neovascularizations (CNV) and macular atrophy [5]. Peripheral arterial calcifications may result in peripheral arterial disease, gastric bleeding and microvascular brain damage [6,7].

Several proteins are involved in maintaining local and systemic PP_i levels, and disruption in one of these proteins results in increased ectopic calcification [8]. In PXE, more than 300 disease-causing ABCC6 variants have been found, with different effects on the protein [9]. ABCC6 protein is mainly expressed on the basolateral membrane of hepatocytes and is thought to be the main source of systemic PP_i. The ABCC6 protein is responsible for increasing extracellular ATP, which is converted to PP_i and AMP [2]. PP_i levels therefore seem to be the causal link between ABCC6 variants and the multi-organ calcification observed in PXE. However, currently there are no data available on how ABCC6 genotype affects plasma PP_i levels. The present study therefore aimed to compare plasma PP_i between a large cohort of PXE patients and controls, and to investigate arterial and ophthalmological phenotypes of PXE with special emphasis on any association between genotype and plasma PP_i levels of the PXE patients who had biallelic pathogenic ABCC6 mutations.

2. Materials and Methods

2.1. Participants

PXE patients were recruited from the Dutch Expertise Center for PXE in the University Medical Center Utrecht, the Netherlands. Controls were recruited from the acquaintances of the PXE patients, excluding first and second-degree relatives. All patients had a clinical diagnosis of PXE based on the criteria of Plomp et al. [4]. In short, patients had to have two of the following three criteria: skin involvement (pseudoxanthomas), eye involvement (peau d'orange and/or angioid streaks), or genetic confirmation (biallelic variants in the ABCC6 gene). For this study, blood was collected for PP_i analysis, and clinical and molecular data from regular care were used (genetics, CT scans, exercise ankle-brachial index, skin photography, ophthalmological examination and imaging). This cross-sectional study was conducted in adherence to the tenets of the Declaration of Helsinki and approved by the medical ethical review board of the University Medical Center Utrecht (IRB# 18-767, 16-622). All participants gave written informed consent for blood collection and all the PXE patients gave written informed consent for the use of their medical files for research purposes.

2.2. Genotyping

Genomic DNA was isolated from whole blood. All ABCC6 exons and the flanking intron sequences were analyzed as part of the genetic screening for regular clinical care. Sanger sequencing was performed to identify rare sequence variants and small deletions and insertions, and multiplex ligation-dependent probe amplification (MLPA) was performed to screen for larger deletions in the ABCC6 gene (reference sequence NM_001171.5, MLPA kit P092B (<https://www.mrcholland.com/>), accessed 14 January 2021). Specific primers were used to avoid the amplification of ABCC6 pseudogenes ψ 1 and ψ 2 [10]. The pathogenicity of all ABCC6 variants was estimated based on the Sherloc criteria [11], a refinement of the guidelines for variant classification of the American College of Medical Genetics and Genomics Association for Molecular Pathology, and classified as benign (class 1), likely benign (class 2), variant of unknown significance (VUS, class 3), likely pathogenic (class 4) or pathogenic (class 5), as previously described [12]. Patients with benign and likely benign variants were excluded from the analysis. VUS with a tendency

towards benign or pathogenic, as based on the Sherlock criteria [11], were classified as such. Since all patients had a confirmed clinical diagnosis of PXE, based on [4], we included patients with a VUS in our analyses. Variants were classified as truncating (nonsense, out-of-frame insertions or deletions, splice site variants that result in a frameshift and deletions of the whole *ABCC6* gene) and non-truncating (missense variants, in-frame insertions or deletions and splice site variants that result in the lack of an in-frame exon), and patients were classified as having two truncating variants, a mixed genotype of one truncating and one non-truncating variant, or two non-truncating variants.

2.3. Blood Collection and PP_i Analysis

Blood was collected in 4.5 mL CTAD vacutainers (BD, 0.11 M buffered trisodium citrate solution, 15 M theophylline, 3.7 M adenosine and 0.198 M dipyridamole). 50 μ L of a 15% K3-ethylenediaminetetraacetic acid (EDTA) solution was added and the tubes were centrifuged for 15 min ($1000\times g$, 4 °C). Blood plasma was transferred to a Centriscart ultrafiltration tube (300 kDa, Sartorius, Göttingen, Germany), centrifuged for 30 min ($2200\times g$, 4 °C) and the filtered plasma was stored at -80 °C until PP_i analysis. Plasma PP_i concentrations were determined as previously described [2]. In short, PP_i was converted into ATP using ATP sulfurylase in the presence of excess adenosine 5'-phosphosulfate (APS). For each 10 μ L of plasma, 70 μ L of a mixture containing 32 mU ATP sulfurylase (ENZ-353; ProSpec, East Brunswick, NJ, USA), 16 μ mol/L APS (A5508; Sigma-Aldrich, St. Louis, MO, USA), 80 μ mol/L $MgCl_2$, and 50 mmol/L HEPES (pH 7.4) was added. Following incubation at 37 °C for 30 min, ATP sulfurylase was inactivated at 90 °C for 10 min. Generated ATP was quantified using the ATP-monitoring reagent BacTiter-Glo (G8230; Promega, San Luis Obispo, CA, USA). An equal volume of BacTiter-Glo reagent was added to the samples. Bioluminescence was determined in a microplate reader (EnSpire Multimode Reader; PerkinElmer, Waltham, MA, USA). Each sample was measured twice in triplicates.

2.4. Arterial Phenotypes

2.4.1. Arterial Calcification

Arterial calcification mass was measured on unenhanced low dose (< 3 mSv for a 70 kg adult), whole body CT scanners (Siemens or Philips, mAs dependent on body weight, 100 or 120 kVp, slice thickness < 1 mm which were resampled to 5 mm slices with 4 mm increment) in the carotid siphon, common carotid artery, coronary arteries, thoracic and abdominal aorta, iliac arteries, and femoral and crural arteries. Arterial calcification was defined as hyperdense arterial wall lesions with a density above 130 Hounsfield Units (HU). Calcification mass scores were computed as the product of the volume of the lesion in ml and the mean attenuation in HU. A peripheral artery score was calculated as the sum of the femoral and crural arteries, and a total arterial calcification mass score was calculated as the sum of all different arterial beds.

2.4.2. Ankle-Brachial Index

The ankle-brachial index (ABI) after a treadmill test was used to measure PAD. To calculate the ABI, systolic blood pressure was measured in the left and right brachial arteries, the tibial posterior arteries and the dorsal pedal arteries. During the treadmill test, patients were encouraged to walk on a treadmill with a 10% slope and a speed of 3.5 km/h for 6 min. Patients who stopped prematurely due to claudication were encouraged to continue walking as soon as possible. During recovery, the ABI was measured for 10 min in a supine position. The lowest value of these ABI measurements was used as the exercise ABI. The ABI measurements were performed by experienced technicians. PAD was defined as an ABI < 0.90 . Patient-reported claudication was measured with the Fontaine classification and patients were classified as having no PAD (ABI > 0.90), asymptomatic PAD (ABI < 0.90 without claudication) and symptomatic PAD (ABI < 0.90 with claudication).

2.5. Ophthalmological Phenotypes

All patients underwent routine ophthalmological examination, including best-corrected visual acuity (BCVA), macular spectral domain optical coherence tomography (SD-OCT), fundus autofluorescence (FAF), near-infrared reflectance imaging (NIR) (all Spectralis HRA-OCT, Heidelberg Engineering, Heidelberg, Germany) and color fundus photography (FF 450 plus, Carl Zeiss Meditec AG, Jena, Germany).

2.5.1. Length of Angioid Streaks

The length of angioid streaks on 55° near infrared (NIR) imaging was used as a proxy for the extent of Bruch's membrane calcification, as previously described [5]. The length of the longest angioid streak from the center of the optic disc to the retinal periphery was measured and graded into four zones: zone 1 (<3 mm from the center of the optic disc), zone 2 (3–6 mm), zone 3 (6–9 mm) and zone 4 (>9 mm).

2.5.2. Macular Phenotype

The presence of CNV and the severity of macular atrophy were scored in both eyes by three experienced graders (SR, RvL, JOvN). The presence of (in)active CNV was based on assessment of SD-OCT, fundus photography and fluorescein or indocyanine green angiography. The presence of macular atrophy was based on FAF, SD-OCT, color fundus photography and NIR. The largest atrophic area was graded as 'no atrophy', 'mild atrophy' (<twice the area of the optic disc) or 'severe atrophy' (> twice the area of the optic disc). An atrophic zone surrounding an (in)active CNV was considered independent of macular atrophy. BCVA was measured on Snellen charts or Early Treatment of Diabetic Retinopathy Study (ETDRS) charts and converted to the logarithm of the minimum angle of resolution (logMAR).

2.6. In Vivo Expression of ABCC6 Protein in Mouse Hepatocytes

Animal protocols were approved by the Food Chain Safety and Animal Health Directorate of the Government Office of Pest County, Hungary (XIV-I-001/707-4/2012). ABCC6-expressing liver samples were obtained from 12-week-old *Abcc6*^{-/-} female mice by hydrodynamic tail vein injection (HTVI) of ABCC6 in pLIVE plasmid (Mirus Bio, Madison, WI, USA) as described [9]. Briefly, wild-type and mutant ABCC6 variants' cDNA were cloned into pLIVE expression plasmid (Mirus Bio, Madison, WI, USA), and each animal was given 70 µg of the construct dissolved in 2 mL of sterile saline, injected in the lateral tail vein in no more than 5 s, achieving the necessary hydrodynamic shock that creates a temporary disruption in the membrane of hepatocytes. Four days later, the mice were euthanized by an overdose of anesthetic (intraperitoneal injection of tiletamine/zolazepam (30 mg/kg, Zoletil, Virbac, France), xylazine (12.5 mg/kg, Primazin, Alfasan, The Netherlands) and butorphanol (3 mg/kg, Butomidor, Richter Pharma, Austria), liver lobes harvested and snap-frozen in 2-methylbutane cooled by liquid nitrogen. Immunohistochemistry was performed as previously described [9].

2.7. Statistical Analysis

Characteristics are presented as mean ± standard deviation for normally distributed continuous variables, median (interquartile range (IQR)) for non-parametric distributed continuous variables and number (%) for categorical variables. For the ophthalmological phenotypes, data for the right eye were used for descriptive and regression analyses. If imaging of the right eye was not assessable, the left eye was used. The correlation between plasma PP_i and continuous outcome measures was tested with the Pearson correlation.

Linear regression models were built with genotype or the individual phenotypes as the determinant and plasma PP_i as the outcome, and adjusted for age and sex. Log₁₀ transformation was performed on the calcification mass scores. The models including arterial calcification mass scores were additionally adjusted for differences in scanner and settings

since this has been shown to affect calcification mass scores [13,14]. A p -value < 0.05 was regarded as statistically significant. All analyses were performed in RStudio version 1.1.456.

3. Results

In total, 207 PXE patients from 175 families and 45 controls were included in this study. Age was similar between the groups (PXE: 55 ± 13 vs. controls 52 ± 16 years, $p = 0.23$), but more of the PXE patients were females (125 (60%) vs. 82 (40%) males, $p = 0.02$). In all 207 patients and 45 controls, PP_i was measured. In addition, 189 patients underwent CT scanning, all patients underwent an exercise ABI measurement and 193 patients underwent an ophthalmological examination. Of the 207 patients, 192 were found to have biallelic pathogenic *ABCC6* mutations.

3.1. Determinants of PP_i in PXE

The PXE patients had lower plasma PP_i than the controls (0.53 ± 0.15 vs 1.13 ± 0.29 μM , $p < 0.01$, Table 1). In the PXE patients, plasma PP_i was correlated with age (β : 0.05 μM , 95% CI: 0.03 – 0.06 per 10 years, $r = 0.40$, $p < 0.01$). The female PXE patients had slightly but significantly higher PP_i than the males (0.51 ± 0.13 in males vs. 0.55 ± 0.17 μM in females, $p = 0.03$, Figure 1). The difference between males and females remained statistically significant after adjustment for age (β : 0.06 μM , 95% CI: 0.02 – 0.10).

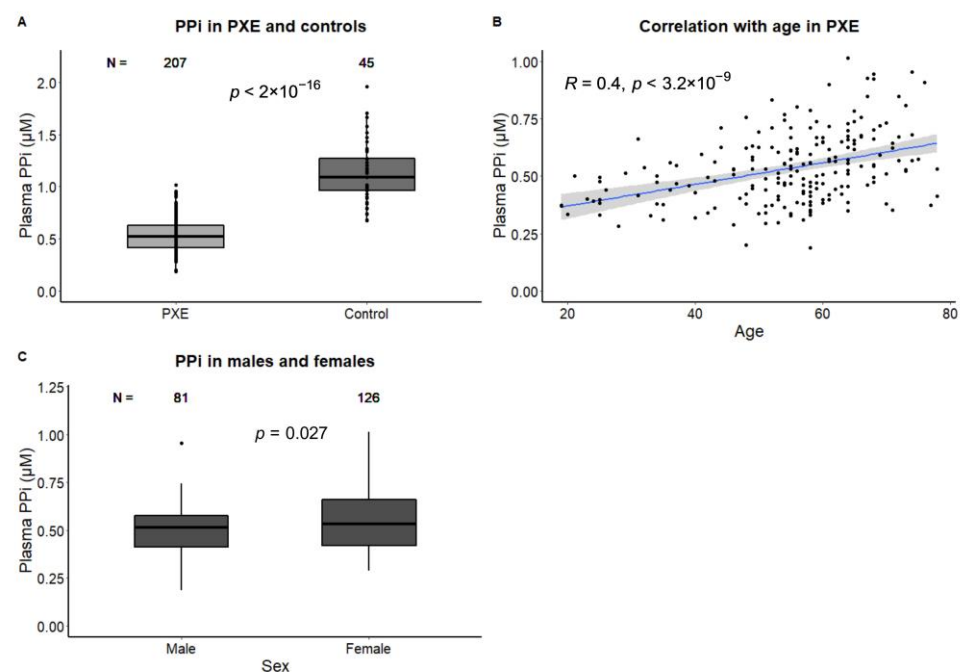


Figure 1. Inorganic pyrophosphate in PXE and controls. Plasma PP_i is approximately 60% lower in PXE patients than in controls (A). Plasma PP_i is correlated with age in PXE (B) and female PXE patients have slightly higher PP_i (C). Data were analyzed with Student's t -test (categorical variables) or the Pearson correlation (continuous variables). A p -value < 0.05 was regarded as statistically significant.

3.2. Association of PP_i and Arterial Calcification and Function

Higher peripheral and total arterial calcification mass were weakly correlated with higher plasma PP_i ($r = 0.19$, $p < 0.01$, and $r = 0.25$, $p < 0.01$, respectively). However, when adjusted for age and sex, no association between plasma PP_i and peripheral (β : 0.00 μM , 95% CI: -0.02 – 0.02) and total (β : 0.01 , 95% CI: -0.02 – 0.04 μM) arterial calcification mass was found. Patients with PAD ($n = 108$, 52%) had higher plasma PP_i than patients without PAD (0.56 ± 0.16 with PAD vs 0.51 ± 0.15 μM without PAD, $p = 0.01$), but this difference attenuated after adjustment for age and sex (β : 0.02 μM , 95% CI: -0.02 – 0.06 , Table 2).

Table 1. Patient characteristics.

Characteristic	PXE (<i>n</i> = 207)	Controls (<i>n</i> = 45)	<i>p</i> -Value
Age, years	55 ± 13	53 ± 16	0.21
Sex, female	126 (61%)	19 (42%)	0.02
PP _i , μM	0.53 ± 0.15	1.13 ± 0.29	<0.01
Genotype	<i>n</i> = 192		
Two truncating, <i>n</i> (%)	116 (56%)		
Mixed, <i>n</i> (%)	71 (34%)		
Two non-truncating, <i>n</i> (%)	14 (7%)		
Arterial calcification	<i>n</i> = 189		
Peripheral, mass score	589 (82–1932)		
Total body, mass score	1518 (186–4178)		
Arterial functioning	<i>n</i> = 207		
Ankle brachial index	0.89 (0.63–1.04)		
Peripheral arterial disease, <i>n</i> (%)	108 (52%)		
Fontaine classification			
No peripheral arterial disease, <i>n</i> (%)	98 (47%)		
Asymptomatic, <i>n</i> (%)	67 (32%)		
Symptomatic, <i>n</i> (%)	42 (20%)		
Ophthalmology	<i>n</i> = 193		
Length of angioid streaks			
<3 mm from optic disc	1 (0.5%)		
3–6 mm from optic disc	38 (20%)		
6–9 mm from optic disc	60 (32%)		
>9 mm from optic disc	87 (47%)		
Choroidal neovascularization, <i>n</i> (%)	119 (62%)		
Macular atrophy, <i>n</i> (%)			
Mild	25 (13%)		
Severe	29 (15%)		
Visual acuity, LogMar	0.10 (0.00–0.70)		

Data are shown as mean ± SD, median [IQR] or *n* (%). Differences between the PXE patients and controls were analyzed with Student's *t*-test (age, PP_i) or the χ^2 test (sex). A *p*-value < 0.05 was regarded as statistically significant. The length of angioid streaks was missing in seven PXE patients. In two patients, 55 near-infrared reflectance imaging was missing, while in five patients severe scarring or atrophy impaired reliable grading.

3.3. Association of PP_i and Ophthalmological Phenotypes

Patients with CNV (*n* = 119, 62%), had higher plasma PP_i than patients without CNV (0.57 ± 0.15 with CNV vs. 0.48 ± 0.14 μM in patients without CNV, *p* < 0.01) and worse visual acuity was weakly correlated with higher PP_i (*r* = 0.19, *p* < 0.01, Figure 2). When adjusted for age and sex, the presence of CNV was associated with higher plasma PP_i (β : 0.06 μM, 95% CI: 0.01–0.11, Table 2). No significant association between PP_i and the other ophthalmological phenotypes was found.

3.4. Association of PP_i and ABCC6 Genotype

Of the 207 patients, 192 were included in the ABCC6 genotype and plasma PP_i level correlation analysis (for a detailed list, see Supplementary Table S1). ABCC6 variants were classified as truncating or non-truncating. Accordingly, three groups of patients were formed: those with truncating mutations on both chromosomes (*n* = 121), those with two non-truncating mutations (*n* = 10), and a third group who had one truncating and one non-truncating ABCC6 mutation (*n* = 61).

Table 2. Association between plasma PP₁ and different arterial and ophthalmological phenotypes.

Variable	Age and Sex Adjusted β (95% Confidence Interval)
Arterial calcification mass	
Peripheral arteries	0.00 (−0.02;0.02)
Total body	0.01 (−0.02;0.04)
Arterial functioning	
Ankle brachial index	0.02 (−0.06;0.09)
Peripheral arterial disease	0.02 (−0.02;0.06)
Fontaine classification	0.00 (−0.03;0.03)
Ophthalmology	
Angioid streaks	0.01 (−0.02;0.03)
Choroidal neovascularization	0.06 (0.01;0.11) *
Macular atrophy	0.01 (−0.02;0.04)
Visual acuity	−0.00 (−0.04;0.03)

Linear regression models were built with one of the above-mentioned variables as the determinant and plasma PP₁ in μM as the outcome. Models were adjusted for age and sex. Genetics = two truncating, mixed and two non-truncating variants. * = p -value < 0.05.

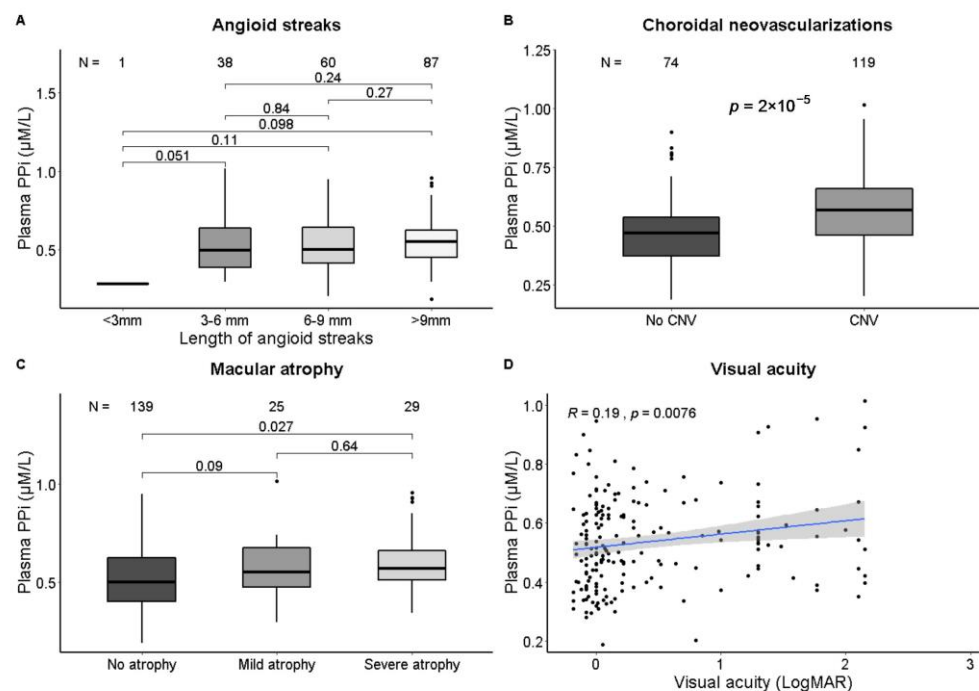


Figure 2. Correlation of plasma PP₁ and ophthalmological phenotypes. Plasma PP₁ is correlated with the presence of choroidal neovascularizations (B). Patients with severe macular atrophy have higher PP₁ than patients without macular atrophy (C), and worse visual acuity is weakly correlated with higher PP₁ (D). No significant correlation with the length of angioid streaks (A) was found. Data were analyzed with Student’s *t*-test (categorical variables) or the Pearson correlation (continuous variables). A p -value < 0.05 was regarded as statistically significant.

In our PXE cohort, a total of 81 non-truncating missense alleles were identified: 61 of these were in the ‘mixed’ group (i.e., the other allele had a truncating mutation), and the remaining 20 were the alleles of 10 patients carrying missense mutations on both chromosomes. Altogether we found 34 different missense mutations, which represented a spectrum with high variety.

No significant difference was found between the plasma PP_i levels of the groups with two truncating *ABCC6* alleles, or two non-truncating alleles, or those who had one truncating and one non-truncating allele (Figure 3A).

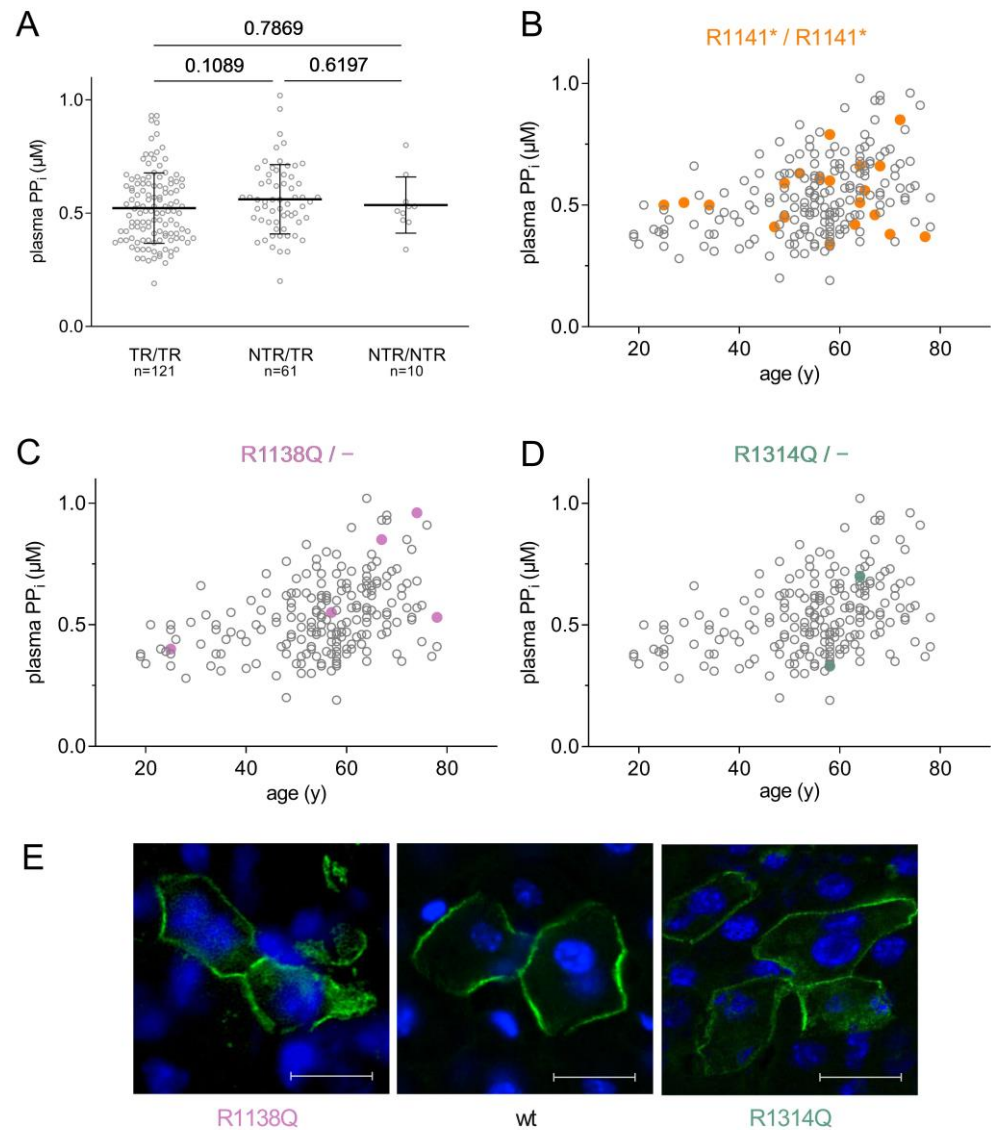


Figure 3. Correlation *ABCC6* genotype and plasma PP_i . (A) Plasma PP_i does not correlate with *ABCC6* genotype. *ABCC6* variants were classified as truncating or non-truncating. Accordingly, three groups of patients were formed: those with truncating mutations on both chromosomes (TR/TR); those with two non-truncating mutations (NTR/NTR), and a third group who had one truncating and one non-truncating *ABCC6* mutation (TR/NTR). (B) Plasma PP_i levels of patients homozygous for R1141* vary between 0.35 and 0.85 μ M. R1141* homozygotes are shown on the age vs. plasma PP_i plot as orange dots, R1141* homozygous patients from the same family are indicated by squares. (C) Patients with the non-truncating R1138Q mutation on one allele and TR on the other allele are highlighted in purple on the age vs. plasma PP_i plot; (D) patients with the non-truncating R1314Q mutation on one allele and TR on the other allele are highlighted in green. (E) Representative images of the subcellular localization of R1138Q, wt and R1314Q *ABCC6* protein variants in vivo in the liver of *Abcc6*^{-/-} mice [10]; *ABCC6* protein is shown in green, and nuclei stained by DAPI are shown in blue (scale bar = 20 μ m).

We analyzed a few mutations in detail: for instance, the mutation R1141* was present in homozygous form in 21 (10.9%) of the 192 PXE patients, making R1141*/R1141* the

most common ABCC6 genotype in the cohort examined. This high prevalence is not unexpected, since this mutation is quite common in the European PXE population [15–17]. It results in a C-terminally truncated ABCC6 lacking a large part of the protein, rendering it nonfunctional, and decreasing its expression to undetectable levels [18]. Figure 3B highlights patients homozygous for R1141* on the age vs. plasma PP_i plot, revealing that plasma PP_i concentrations observed in these patients varied widely (between 0.35 and 0.85 μM) and that the ABCC6 genotype of these patients apparently did not account for these differences. Even the three patients from the same family (shown as squares) had different plasma PP_i.

We studied the cellular localization of two missense mutants by overexpressing the human ABCC6 protein variants in the liver of *Abcc6*^{-/-} mice [9]. A strength of this experimental approach is that the expression happens in vivo in the native environment of the liver, in the tissue and cell type where ABCC6 protein is physiologically present. In addition to confirming protein expression, this method can also establish the subcellular localization of a given mutant in its physiological conditions. We have shown earlier that wild-type human ABCC6 protein is expressed in the basolateral plasma membrane of the hepatocytes of the mouse liver (see Figure 3E, central panel; this is a criterion of being physiologically active), while some mutants show complete or partial intracellular retention [9,19]. Missense mutant R1138Q was found in five patients of the mixed group, i.e., each patient carried this mutation on one allele and a truncated one on the other allele. The cellular localization of this mutant showed partial intracellular retention, as shown on Figure 3E, left panel, in harmony with our earlier observation [9]. The plasma PP_i level varied in these five patients between 0.40 μM to 0.96 μM, lacking any apparent correlation between this specific missense mutation and the plasma PP_i measured.

The mutation R1314Q, which also gave rise to a partially mislocalized ABCC6 protein, was found in a PXE patient with 0.35 ± 0.03 μM plasma PP_i concentration, and one who, in contrast, had 0.7 ± 0.04 μM of plasma PP_i (Figure 3E, right panel). The difference is striking, even though these patients' ABCC6 genotypes are similar, with R1314Q on one allele, and a truncating mutation on the other.

4. Discussion

In this large cohort of PXE patients, we show that PP_i levels are approximately 60% lower than those of a control population, which confirms that PP_i is involved in the pathogenesis of PXE. PP_i levels were positively correlated with increasing age and were slightly higher in females. Similar results have been published recently, independent of the present study, which support these correlations being solid, the results coming from two different cohorts of 207 patients (present study) and 107 patients [20].

More importantly, we found that plasma PP_i levels were not associated with disease severity in PXE. Only a small association between plasma PP_i and CNV was found, and other ophthalmological outcomes were not associated with plasma PP_i. In the recent publication of Leftheriotis et al. also no association between plasma PP_i and lower limb arterial calcification was found [20], comparable to our results concerning PP_i and peripheral artery calcification score. Total body arterial calcification, as well as ophthalmological outcomes, were not studied by these authors. Contrary to PP_i, age seems to be the most important determinant for disease severity in PXE. More ectopic calcification, as seen in older patients, leads to more need for inhibitors of it, of which PP_i is one of the most important, but as we did not find an association between PP_i and disease severity it remains difficult to explain the association between PP_i and age that we and others have found.

Our findings add to a growing body of evidence showing that both systemic and local factors contribute to the pathophysiology of PXE. The ABCC6 protein is thought to account for approximately 60% of circulating extracellular PP_i [2]. Although studies of PXE patients and mouse models consistently show reduced systemic PP_i [2,21,22], PXE is characterized by large heterogeneity of symptoms in patients with the same pathogenic variants and even within families [23]. We recently showed that patients with two truncating variants in the

ABCC6 gene have more severe arterial calcification and longer angioid streaks than patients with a mixed genotype, which emphasizes the role of ABCC6 in ectopic calcification. This, however, did not translate to more severe clinical consequences [12].

An interesting study has been published recently regarding the genotype, disease phenotype and plasma PP_i of patients with inborn calcification disorders caused by inactivating mutations of ectonucleotide pyrophosphatase/phosphodiesterase 1 (ENPP1) encoding the nuclease acting upstream to ABCC6 protein [24] (see Figure 4A). Mutations in ENPP1 are responsible for the severe disorder generalized arterial calcification in infancy (GACI). In this study, two individuals diagnosed with PXE were found to have biallelic mutations in their ENPP1 gene, yet surprisingly these patients presented a more favorable clinical outcome of PXE phenotype. Their plasma PP_i concentrations were substantially decreased, similar to the two individuals who had biallelic mutations in their ENPP1 genes and the much more severe phenotype of GACI. This observation also suggests that the relationship between reduced plasma PP_i and ectopic calcification symptom severity may not be as direct as previously thought.

In the present study we have found that even though biallelic ABCC6 mutations do decrease plasma PP_i level, the highly variable plasma PP_i concentrations measured in our PXE cohort cannot be attributed to the specific type of ABCC6 mutations these individuals harbor, even though ABCC6 protein has a key role in the metabolic pathway responsible for approximately 60% of circulating extracellular PP_i [2] (see Figure 4A). One of the strengths of the present study is the large number of patients included, with both detailed genotypic characterization and plasma PP_i data available.

The lack of association between genotype and plasma PP_i level in PXE revealed by the present study is rather unexpected, since one would have predicted that several missense ABCC6 variants preserved decreased residual activity, thus providing higher plasma PP_i than found in the truncating/truncating group. However, we detected no difference between the PP_i levels of patients with one or with two missense mutations as compared with the values of the truncating/truncating group. Furthermore, our finding that the same mutation is accompanied by very different plasma PP_i (see Figure 3) also mitigates against the above assumption. Our findings collectively suggest the existence of additional factors perturbing the expected associations between genotype and plasma PP_i, and between plasma PP_i and disease severity. Our hypothesis on the role of potential factors is summarized in Figure 4. ABCC6 protein in the liver is thought to be the main source of extracellular ATP, which is subsequently converted to PP_i and AMP by ENPP1 [2]. Factors potentially perturbing the genotype–plasma PP_i correlation are: (i) the level of ABCC6 protein expression in the liver, controlled by e.g., oxidative stress [25,26]; and (ii) the activity of additional proteins involved in generation (ANK [27] and ENPP1) or removal (NT5E and TNAP) of extracellular PP_i, which may significantly influence plasma PP_i. In addition, there is competition for ATP in the circulation: ENPP1 is the only nuclease producing PP_i from ATP, while ectonucleoside triphosphate diphosphohydrolase (eNTPD) enzymes ‘consume’ ATP without generating PP_i [28]. This is another perturbing effect reducing the ATP substrate concentration available for ENPP1.

Furthermore, PP_i is not the sole possible inhibitor of ectopic calcification, and disease severity in PXE may be influenced by other calcification inhibitors, e.g., fetuin A [29]. We also have to consider the roles of environmental factors like diet (some food contains PP_i as an additive), or smoking, which could enhance disease severity.

Utilizing animal models, it was found that although reduced plasma PP_i is a major cause of ectopic mineralization in PXE, it is not the only factor that prevents ectopic calcification [30,31]. In spite of this complex picture, several therapies to increase PP_i are currently under development for the treatment of PXE and related disorders. Orally delivered PP_i has been shown to increase plasma PP_i in humans and mice, and to inhibit cardiac calcification and calcification of the vibrissae, kidneys and arteries of the legs in mice [22]. These latter results further support the causal role of reduced PP_i in PXE. The recombinant ENPP1 enzyme INZ-701 was shown to increase plasma PP_i, inhibit cardiac

and aortic calcification and increase survival in *Enpp1*^{-/-} mice [32], and in addition it also increased plasma PP_i and partially prevented calcification in *Abcc6*^{-/-} mice [33]. Inhibition of TNAP also reduced calcification in *Abcc6*^{-/-} mice [34]. Finally, we have demonstrated that the bisphosphonate etidronate, a stable analogue of PP_i, inhibits systemic arterial calcification in PXE patients [35].

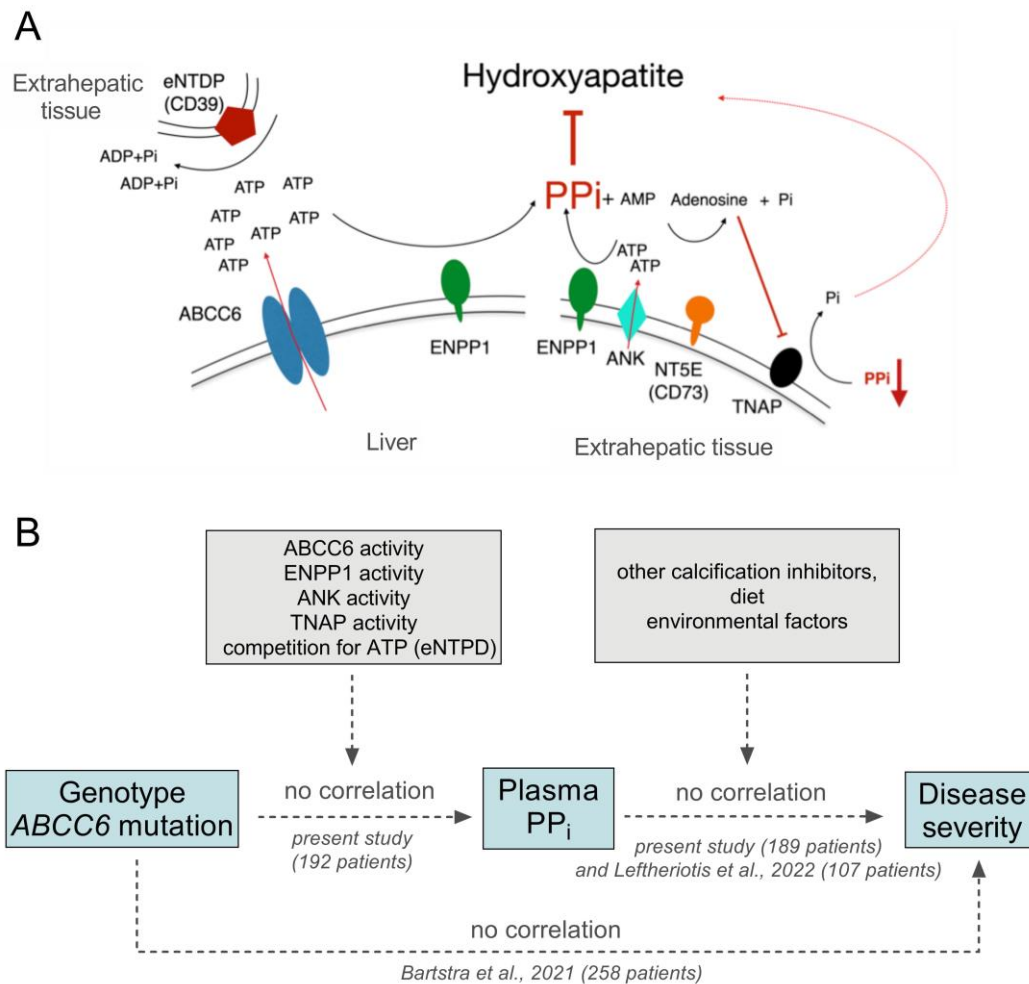


Figure 4. Crucial players of plasma pyrophosphate homeostasis, and factors modifying plasma pyrophosphate level and disease severity in pseudoxanthoma elasticum. **(A)** The activity of ABCC6 protein and ENPP1 in the liver are responsible for approximately 60% of extracellular PP_i in the circulation. In extrahepatic tissues, human progressive ankylosis (ANKH) protein, similarly to ABCC6 protein, facilitates ATP release from cells, while tissue-nonspecific alkaline phosphatase (TNAP) cleaves PP_i, thus lowering its concentration. AMP is hydrolyzed by NT5E (CD73) to inorganic phosphate and adenosine, and the latter down-regulates TNAP expression, thus controlling its activity and increasing plasma PP_i. Ectonucleoside triphosphate diphosphohydrolase enzymes (eNTPDs) compete for ATP with ENPP1. **(B)** Left: the expression and activity of ABCC6 protein, ANK and ENPP1 all contribute to increasing plasma PP_i, while TNAP, on the other hand, decreases it. Competition for extracellular ATP in plasma by ENPP1 and eNTPDs may also influence pyrophosphate homeostasis. **(B)** Right: other calcification inhibitors, which exert their effect independent of plasma PP_i concentration, as well as dietary and environmental factors, can also impact calcification symptoms of PXE.

5. Conclusions

Our results support that PXE patients have approximately 60% reduced plasma PP_i levels when compared with controls. Plasma PP_i levels were correlated with increasing

age and were higher in female PXE patients. Contrary to expectations, no clear association between plasma PP_i levels and disease severity was found in PXE. Another unexpected finding of our study is that no correlation between ABCC6 genotype and plasma PP_i level was found in the 192 pseudoxanthoma elasticum patients with known pathogenic phenotypes. Our findings should trigger future studies of the role of PP_i in disease progression, and possible genetic or environmental modifiers, which might shed more light on the complex pathophysiology of PXE.

Supplementary Materials: The following supporting information can be downloaded at: <https://www.mdpi.com/article/10.3390/jcm12031047/s1>, Table S1 detailing ABCC6 genotype, age, sex and plasma PP_i of PXE patients.

Author Contributions: E.K.: measured plasma pyrophosphate, expressed human ABCC6 protein mutants in mouse liver, analyzed data, drafted the manuscript, J.W.B.: measured vascular complications, collected clinical data, analyzed data, drafted the manuscript, P.A.d.J.: analyzed data, revised the manuscript, W.P.T.M.M.: analyzed data, revised the manuscript, K.F.: measured plasma pyrophosphate, revised the manuscript, N.T.: measured plasma pyrophosphate, revised the manuscript, V.P.: measured plasma pyrophosphate, expressed human ABCC6 protein mutants in mouse liver, revised the manuscript, S.R.: collected ocular measurements, analyzed data, drafted the manuscript, J.O.-v.N.: analyzed data, revised the manuscript, R.v.L.: analyzed data, revised the manuscript, A.V.: designed experiments, analyzed data, wrote and revised the manuscript, W.S.: conceived the idea, analyzed data, wrote and revised the manuscript. All authors have read and agreed to the published version of the manuscript.

Funding: This work was supported by the National Research, Development and Innovation Office of Hungary grants: OTKA 127957,127933 (AV); PD-OTKA 128003 and 123859 (VP and NT, respectively).

Institutional Review Board Statement: This cross-sectional study was conducted in adherence to the tenets of the Declaration of Helsinki and approved by the medical ethical review board of the University Medical Center Utrecht (IRB# 18-767, 16-622). Animal protocols were approved by the Food Chain Safety and Animal Health Directorate of the Government Office of Pest County, Hungary (XIV-I-001/707-4/2012).

Informed Consent Statement: All participants gave written informed consent for blood collection and all PXE patients gave written informed consent for the use of their medical files for research purposes.

Data Availability Statement: The data presented in this study are available in Supplementary Table S1.

Acknowledgments: We kindly thank all patients and the contributions of I. Klaassen and C. Joosten (research nurses). We thank Olivier Le Saux for the microscopy image of the missense ABCC6 protein variant R1138Q.

Conflicts of Interest: AV is co-inventor on patent applications related to the use of pyrophosphates for therapeutic applications. Application NL20117471, entitled ‘Oral Pyrophosphate For Use In Reducing Tissue Calcification’, is continued as US 16/333,856 and EP17781568.5. Two subsequent patent applications have been filed for improved pyrophosphate salts which improve tolerability and bioavailability: NL2023491 and US 63/091,467, and AV is owner of shares in Pyrogenyx Inc. The other authors declare no conflict of interest.

References

1. Evrard, S.; Delanaye, P.; Kamel, S.; Cristol, J.-P.; Cavalier, E.; SFBC/SN Joined Working Group on Vascular Calcifications. Vascular Calcification: From Pathophysiology to Biomarkers. *Clin. Chim. Acta* **2015**, *438*, 401–414. [[CrossRef](#)] [[PubMed](#)]
2. Jansen, R.S.; Duijst, S.; Mahakena, S.; Sommer, D.; Szeri, F.; Váradi, A.; Plomp, A.; Bergen, A.A.; Oude Elferink, R.P.J.; Borst, P.; et al. ABCC6-Mediated ATP Secretion by the Liver Is the Main Source of the Mineralization Inhibitor Inorganic Pyrophosphate in the Systemic Circulation-Brief Report. *Arterioscler. Thromb. Vasc. Biol.* **2014**, *34*, 1985–1989. [[CrossRef](#)] [[PubMed](#)]
3. Borst, P.; Váradi, A.; van de Wetering, K. PXE, a Mysterious Inborn Error Clarified. *Trends Biochem. Sci.* **2019**, *44*, 125–140. [[CrossRef](#)] [[PubMed](#)]
4. Plomp, A.S.; Toonstra, J.; Bergen, A.A.B.; van Dijk, M.R.; de Jong, P.T.V.M. Proposal for Updating the Pseudoxanthoma Elasticum Classification System and a Review of the Clinical Findings. *Am. J. Med. Genet. A* **2010**, *152A*, 1049–1058. [[CrossRef](#)]
5. Risseuw, S.; Ossewaarde-van Norel, J.; van Buchem, C.; Spiering, W.; Imhof, S.M.; van Leeuwen, R. The Extent of Angioid Streaks Correlates With Macular Degeneration in Pseudoxanthoma Elasticum. *Am. J. Ophthalmol.* **2020**, *220*, 82–90. [[CrossRef](#)]

6. Kranenburg, G.; de Jong, P.A.; Mali, W.P.; Attrach, M.; Visseren, F.L.J.; Spiering, W. Prevalence and Severity of Arterial Calcifications in Pseudoxanthoma Elasticum (PXE) Compared to Hospital Controls. Novel Insights into the Vascular Phenotype of PXE. *Atherosclerosis* **2017**, *256*, 7–14. [[CrossRef](#)]
7. Leftheriotis, G.; Kauffenstein, G.; Hamel, J.F.; Abraham, P.; Le Saux, O.; Willoteaux, S.; Henrion, D.; Martin, L. The Contribution of Arterial Calcification to Peripheral Arterial Disease in Pseudoxanthoma Elasticum. *PLoS ONE* **2014**, *9*, e96003. [[CrossRef](#)]
8. Orriss, I.R.; Arnett, T.R.; Russell, R.G.G. Pyrophosphate: A Key Inhibitor of Mineralisation. *Curr. Opin. Pharmacol.* **2016**, *28*, 57–68. [[CrossRef](#)]
9. Pomozi, V.; Brampton, C.; Fülöp, K.; Chen, L.-H.; Apana, A.; Li, Q.; Uitto, J.; Le Saux, O.; Váradi, A. Analysis of Pseudoxanthoma Elasticum-Causing Missense Mutants of ABCC6 in Vivo; Pharmacological Correction of the Mislocalized Proteins. *J. Investig. Dermatol.* **2014**, *134*, 946–953. [[CrossRef](#)]
10. Hu, X.; Plomp, A.; Gorgels, T.; Brink, J.T.; Loves, W.; Mannens, M.; de Jong, P.T.V.M.; Bergen, A.A.B. Efficient Molecular Diagnostic Strategy for ABCC6 in Pseudoxanthoma Elasticum. *Genet. Test.* **2004**, *8*, 292–300. [[CrossRef](#)]
11. Nykamp, K.; Anderson, M.; Powers, M.; Garcia, J.; Herrera, B.; Ho, Y.-Y.; Kobayashi, Y.; Patil, N.; Thusberg, J.; Westbrook, M.; et al. Sherloc: A Comprehensive Refinement of the ACMG-AMP Variant Classification Criteria. *Genet. Med.* **2017**, *19*, 1105–1117. [[CrossRef](#)]
12. Bartstra, J.W.; Risseeuw, S.; de Jong, P.A.; van Os, B.; Kalsbeek, L.; Mol, C.; Baas, A.F.; Verschuere, S.; Vanakker, O.; Florijn, R.J.; et al. Genotype-Phenotype Correlation in Pseudoxanthoma Elasticum. *Atherosclerosis* **2021**, *324*, 18–26. [[CrossRef](#)]
13. Gräni, C.; Vontobel, J.; Benz, D.C.; Bacanovic, S.; Giannopoulos, A.A.; Messerli, M.; Grossmann, M.; Gebhard, C.; Pazhenkottil, A.P.; Gaemperli, O.; et al. Ultra-Low-Dose Coronary Artery Calcium Scoring Using Novel Scoring Thresholds for Low Tube Voltage Protocols—a Pilot Study. *Eur. Heart J. Cardiovasc. Imaging* **2018**, *19*, 1362–1371. [[CrossRef](#)] [[PubMed](#)]
14. Willeminck, M.J.; Vliegenthart, R.; Takx, R.A.P.; Leiner, T.; Budde, R.P.J.; Bleys, R.L.A.W.; Das, M.; Wildberger, J.E.; Prokop, M.; Bult, N.; et al. Coronary Artery Calcification Scoring with State-of-the-Art CT Scanners from Different Vendors Has Substantial Effect on Risk Classification. *Radiology* **2014**, *273*, 695–702. [[CrossRef](#)] [[PubMed](#)]
15. Chassaing, N.; Martin, L.; Mazereeuw, J.; Barrié, L.; Nizard, S.; Bonafé, J.-L.; Calvas, P.; Hovnanian, A. Novel ABCC6 Mutations in Pseudoxanthoma Elasticum. *J. Investig. Dermatol.* **2004**, *122*, 608–613. [[CrossRef](#)] [[PubMed](#)]
16. Shi, Y.; Terry, S.F.; Terry, P.F.; Bercovitch, L.G.; Gerard, G.F. Development of a Rapid, Reliable Genetic Test for Pseudoxanthoma Elasticum. *J. Mol. Diagn.* **2007**, *9*, 105–112. [[CrossRef](#)] [[PubMed](#)]
17. Pfendner, E.G.; Vanakker, O.M.; Terry, S.F.; Vourthis, S.; McAndrew, P.E.; McClain, M.R.; Fratta, S.; Marais, A.; Hariri, S.; Coucke, P.J.; et al. Mutation Detection in the ABCC6 Gene and Genotype–Phenotype Analysis in a Large International Case Series Affected by Pseudoxanthoma Elasticum. *J. Med. Genet.* **2007**, *44*, 621–628. [[CrossRef](#)]
18. Hu, X.; Peek, R.; Plomp, A.; Brink, J.T.; Scheffer, G.; van Soest, S.; Leys, A.; de Jong, P.T.V.M.; Bergen, A.A.B. Analysis of the Frequent R1141X Mutation in the ABCC6 Gene in Pseudoxanthoma Elasticum. *Investig. Ophthalmol. Vis. Sci.* **2003**, *44*, 1824–1829. [[CrossRef](#)]
19. Pomozi, V.; Le Saux, O.; Brampton, C.; Apana, A.; Iliás, A.; Szeri, F.; Martin, L.; Monostory, K.; Paku, S.; Sarkadi, B.; et al. ABCC6 Is a Basolateral Plasma Membrane Protein. *Circ. Res.* **2013**, *112*, e148–e151. [[CrossRef](#)]
20. Leftheriotis, G.; Navasiolava, N.; Clotaire, L.; Durantou, C.; Le Saux, O.; Bendahhou, S.; Laurain, A.; Rubera, I.; Martin, L. Relationships between Plasma Pyrophosphate, Vascular Calcification and Clinical Severity in Patients Affected by Pseudoxanthoma Elasticum. *J. Clin. Med.* **2022**, *11*, 2588. [[CrossRef](#)]
21. Kozák, E.; Fülöp, K.; Tókési, N.; Rao, N.; Li, Q.; Terry, S.F.; Uitto, J.; Zhang, X.; Becker, C.; Váradi, A.; et al. Oral Supplementation of Inorganic Pyrophosphate in Pseudoxanthoma Elasticum. *Exp. Dermatol.* **2021**, *31*, 14498. [[CrossRef](#)] [[PubMed](#)]
22. Dedinszki, D.; Szeri, F.; Kozák, E.; Pomozi, V.; Tókési, N.; Mezei, T.R.; Merczel, K.; Letavernier, E.; Tang, E.; Le Saux, O.; et al. Oral Administration of Pyrophosphate Inhibits Connective Tissue Calcification. *EMBO Mol. Med.* **2017**, *9*, 1463–1470. [[CrossRef](#)] [[PubMed](#)]
23. Plomp, A.S.; Bergen, A.A.B.; Florijn, R.J.; Terry, S.F.; Toonstra, J.; van Dijk, M.R.; de Jong, P.T.V.M. Pseudoxanthoma Elasticum: Wide Phenotypic Variation in Homozygotes and No Signs in Heterozygotes for the c.3775delT Mutation in ABCC6. *Genet. Med.* **2009**, *11*, 852–858. [[CrossRef](#)] [[PubMed](#)]
24. Ralph, D.; Nitschke, Y.; Levine, M.A.; Caffet, M.; Wurst, T.; Saeidian, A.H.; Youssefian, L.; Vahidnezhad, H.; Terry, S.F.; Rutsch, F.; et al. ENPP1 Variants in Patients with GACI and PXE Expand the Clinical and Genetic Heterogeneity of Heritable Disorders of Ectopic Calcification. *PLoS Genet.* **2022**, *18*, e1010192. [[CrossRef](#)] [[PubMed](#)]
25. de Boussac, H.; Ratajewski, M.; Sachrajda, I.; Köblös, G.; Tordai, A.; Pulaski, L.; Buday, L.; Váradi, A.; Arányi, T. The ERK1/2-Hepatocyte Nuclear Factor 4alpha Axis Regulates Human ABCC6 Gene Expression in Hepatocytes. *J. Biol. Chem.* **2010**, *285*, 22800–22808. [[CrossRef](#)]
26. Abruzzese, V.; Matera, I.; Martinelli, F.; Carosino, M.; Koshal, P.; Milella, L.; Bisaccia, F.; Ostuni, A. Effect of Quercetin on ABCC6 Transporter: Implication in HepG2 Migration. *Int. J. Mol. Sci.* **2021**, *22*, 3871. [[CrossRef](#)] [[PubMed](#)]
27. Szeri, F.; Lundkvist, S.; Donnelly, S.; Engelke, U.F.H.; Rhee, K.; Williams, C.J.; Sundberg, J.P.; Wevers, R.A.; Tomlinson, R.E.; Jansen, R.S.; et al. The Membrane Protein ANKH Is Crucial for Bone Mechanical Performance by Mediating Cellular Export of Citrate and ATP. *PLoS Genet.* **2020**, *16*, e1008884. [[CrossRef](#)]
28. Villa-Bellosta, R. ATP-Based Therapy Prevents Vascular Calcification and Extends Longevity in a Mouse Model of Hutchinson-Gilford Progeria Syndrome. *Proc. Natl. Acad. Sci. USA* **2019**, *116*, 23698–23704. [[CrossRef](#)] [[PubMed](#)]

29. Jahnen-Dechent, W.; Schinke, T.; Trindl, A.; Müller-Esterl, W.; Sablitzky, F.; Kaiser, S.; Blessing, M. Cloning and Targeted Deletion of the Mouse Fetuin Gene. *J. Biol. Chem.* **1997**, *272*, 31496–31503. [[CrossRef](#)]
30. Zhao, J.; Kingman, J.; Sundberg, J.P.; Uitto, J.; Li, Q. Plasma PPI Deficiency Is the Major, but Not the Exclusive, Cause of Ectopic Mineralization in an *Abcc6*^{-/-} Mouse Model of PXE. *J. Investig. Dermatol.* **2017**, *137*, 2336–2343. [[CrossRef](#)]
31. Li, Q.; Huang, J.; Pinkerton, A.B.; Millan, J.L.; van Zelst, B.D.; Levine, M.A.; Sundberg, J.P.; Uitto, J. Inhibition of Tissue-Nonspecific Alkaline Phosphatase Attenuates Ectopic Mineralization in the *Abcc6*^{-/-} Mouse Model of PXE but Not in the *Enpp1* Mutant Mouse Models of GACI. *J. Investig. Dermatol.* **2019**, *139*, 360–368. [[CrossRef](#)] [[PubMed](#)]
32. Albright, R.A.; Stabach, P.; Cao, W.; Kavanagh, D.; Mullen, I.; Braddock, A.A.; Covo, M.S.; Tehan, M.; Yang, G.; Cheng, Z.; et al. ENPP1-Fc Prevents Mortality and Vascular Calcifications in Rodent Model of Generalized Arterial Calcification of Infancy. *Nat. Commun.* **2015**, *6*, 10006. [[CrossRef](#)] [[PubMed](#)]
33. Jacobs, I.J.; Cheng, Z.; Ralph, D.; O'Brien, K.; Flaman, L.; Howe, J.; Thompson, D.; Uitto, J.; Li, Q.; Sabbagh, Y. INZ-701, a Recombinant ENPP1 Enzyme, Prevents Ectopic Calcification in an *Abcc6*^{-/-} Mouse Model of Pseudoxanthoma Elasticum. *Exp. Dermatol.* **2022**, *31*, 1095–1101. [[CrossRef](#)] [[PubMed](#)]
34. Ziegler, S.G.; Ferreira, C.R.; MacFarlane, E.G.; Riddle, R.C.; Tomlinson, R.E.; Chew, E.Y.; Martin, L.; Ma, C.-T.; Sergienko, E.; Pinkerton, A.B.; et al. Ectopic Calcification in Pseudoxanthoma Elasticum Responds to Inhibition of Tissue-Nonspecific Alkaline Phosphatase. *Sci. Transl. Med.* **2017**, *9*, eaal1669. [[CrossRef](#)] [[PubMed](#)]
35. Kranenburg, G.; de Jong, P.A.; Bartstra, J.W.; Lagerweij, S.J.; Lam, M.G.; Ossewaarde-van Norel, J.; Risseeuw, S.; van Leeuwen, R.; Imhof, S.M.; Verhaar, H.J.; et al. Etidronate for Prevention of Ectopic Mineralization in Patients With Pseudoxanthoma Elasticum. *J. Am. Coll. Cardiol.* **2018**, *71*, 1117–1126. [[CrossRef](#)] [[PubMed](#)]

Disclaimer/Publisher's Note: The statements, opinions and data contained in all publications are solely those of the individual author(s) and contributor(s) and not of MDPI and/or the editor(s). MDPI and/or the editor(s) disclaim responsibility for any injury to people or property resulting from any ideas, methods, instructions or products referred to in the content.